

Estimating the Parameters of Small Earthquakes and Their Signals

B. V. Levin^a, E. V. Sasorova^b, S. A. Borisov^a, and A. S. Borisov^a

^a *Institute of Marine Geology and Geophysics, Far East Division, Russian Academy of Sciences, Yuzhno-Sakhalinsk, 693022 Russia*

^b *Institute of Oceanology, Russian Academy of Sciences, Moscow, 117997 Russia*

Received April 29, 2008

Abstract—This study is an attempt at a theoretical synthesis of the following earthquake parameters: the length and volume of the rupture zone, energy, magnitude, energy class, as well as the period and frequency of seismic signals. We have obtained the signal period (T) as a function of event energy (E) for a very broad class of events ranging from large earthquakes to microscopic ruptures (nanoequakes). It is shown for the first time here that earthquake energy is related to the period of the seismic signal in a power-law manner, with the exponent being equal to 6, which finds an explanation within the framework of dimension theory. We have examined a large amount of both onshore and hydroacoustic observations of seismic events of different energy levels. These observations include small seismic events in the frequency range 50–1000 Hz that we were observing in Kamchatka and in the Sakhalin-Kuril region. This has been the basis for deriving the experimental relationship $T = f(E)$, in good agreement with theoretical estimates. We examined the degree of seismic signal attenuation versus frequency and distance to receiver for different media (including composite media); the attenuation incorporates, not only absorption in the medium (intrinsic attenuation), but also geometrical spreading. It is shown that signals at frequencies above 200 Hz are nearly completely attenuated in solids at distances below one kilometer from the source. We propose a formal quantitative criterion for classifying small seismic events into subclasses: small earthquakes (magnitude $1 \leq M \leq 3$, frequency range $3 \leq f \leq 10$ Hz); microearthquakes (magnitude $-4 \leq M \leq 0$, frequency range $20 \text{ Hz} \leq f \leq 170$ Hz), and microscopic ruptures or nanoequakes ($M \leq -5$, frequency $f \geq 200$ Hz). This classification was previously available on a descriptive level only.

DOI: 10.1134/S074204631003005X

INTRODUCTION

In accordance with the current concepts of specialists in earthquake physics and fracture physics, the generation of seismic waves during an earthquake and the radiation of an elastic wave during the appearance of a crack (a set of cracks) are to be treated as phenomena that differ in scale, but which are similar (identical) in their underlying physical mechanisms. Seismologists are well aware of the fact that the entire range of seismic events from micro-earthquakes to disastrous earthquakes covers a range of energy measuring 18 orders, while the period of the associated radiated signals encompasses only 3 orders. It is also a known fact that the energy of an earthquake is a function of the rupture volume where the energy of the seismic event in question is released. Until recently, however, many aspects in the physics of small earthquakes remain debatable, even though these events are of great interest in connection with man-made processes, enhanced measurement accuracy and recording possibilities, and with numerous attempts at interpreting geodynamic phenomena and possible implementation of practical earthquake prediction.

Since small earthquakes are much more frequent than larger events, while their signals bear great total amounts

of information on the seismic process, it follows that the study of the parameters of these earthquakes and the wave propagation from these sources can provide the science and technology community with new evidence on earthquake generation, enabling many practical problems to be attacked. The present study has the following goal: comparing the source parameters of small earthquakes with the characteristics of signals radiated based on an analysis of historical and currently acquired data (including these authors' measurements in the Russian Far East), obtaining a quantitative estimate for the period of seismic signals as a function of the energy of events, and putting forward criteria for the classification of low magnitude earthquakes.

EMPIRICAL RELATIONSHIPS FOR EARTHQUAKE PARAMETERS

The experience accumulated by the seismologists during the last 50 years allows us to highlight several important empirical relationships that involve basic earthquake parameters. Some materials on this theme can be found in the Russian-language collection of translations *Weak Earthquakes* [18], which contains several pioneer studies.

The Japanese seismologist Tsuboi [23] was the first to substantiate and propose an equation that connects earthquake energy E and rupture volume V , viz.,

$$E(\text{ergs}) = 1000V(\text{cm}^3). \quad (1)$$

A similar empirical equation was put forward by M.A. Sadvskii et al. [15] as a result of studies in the after-shock areas of underground nuclear blasts. These authors showed that seismic energy density and the volumes that radiate elastic seismic waves have similar values for crustal earthquakes and underground explosions and can be described by the expression $\log E = \log V + 3$ with dimensions as in (1).

The same reference contains a relationship for estimating the source length from the earthquake rupture volume. It goes without saying that these equations should be viewed as first approximations. Following Sadvskii, we note that the great variety of earthquake slip mechanisms (normal, strike slip, thrust, etc.), as well as differences between rock properties, cannot be left entirely out of consideration. Experience shows, however, that to a first approximation we can safely neglect these parameters.

The publication of V.B. Smirnov [19] gives the widely accepted relationship between earthquake energy and source length L ,

$$E = eL^3, \quad (2)$$

where E is in ergs, the accumulated elastic energy density “ e ” has an average value of 1000 erg/cm^3 , and the source length is in cm. These empirical relationships give a one-to-one correspondence between energy and the size of the volume that radiates elastic waves.

Of great importance for the present study is the relationship between the size of the source (a crack, radiator, or a generator of acoustic waves) and the period of the radiated signal. We have studied extensive data of recorded signals from earthquakes, rock bursts, and geoacoustic emission [16, 27] to find the relationship between the size of the radiating source and signal period in the form

$$L \approx B_1 T^2, \quad (3)$$

where $B_1 = 2500 \text{ m/s}^2$.

The subsequent analysis of the parameters of small earthquakes will be based on an empirical relationship between source energy and the period of radiated wave. Such relationships for earthquakes of magnitude $M > 0$ are given as empirical formulas thanks to notable seismologists [3, 5]:

$$\log T = -0.82 + 0.22M \text{ (Gutenberg and Richter)}, \quad (4)$$

$$\log T = -0.78 + 0.28M \text{ (Kasahara)}. \quad (5)$$

The analysis of earthquake parameters using the independent relationships (1) through (3) can be used to derive the period of radiated signals as a function of earthquake energy. The relationship can then be compared with the empirical relationships (4, 5) after checking and refinement of these. We have refined the relationship that connects source energy to wave period by doing a special

analysis of the publications concerned with small earthquakes followed by experimenting in seismic zones of the Russian Far East to detect very small events by hydroacoustic recording in the field.

A BRIEF ANALYSIS OF OBSERVATIONAL DATA ON SMALL SEISMIC EVENTS

It should be noted that in recent years there has been a growing interest in small seismic events (small earthquakes, microearthquakes and microfractures). At the same time, the recording of these events and the determination of their parameters (magnitude, rupture length, frequency characteristics, etc.), as well as of the relationships connecting these parameters, remains largely problematical.

The signals excited by small sources typically involve high frequencies, hence the signals are rapidly attenuated in solid media, especially in sediments, until they completely die out. However, the low attenuation of these signals in water makes it possible to record them in a water layer by hydroacoustic observational techniques. In this connection it is of interest to estimate seismic signal parameters from hydroacoustic records or from combined seismic and hydroacoustic records. The goal of the present part of this study is to develop a general technique for estimating the energy and frequency parameters of seismic events.

Below we present the main results from instrumental recording of small seismic events using electromechanical and hydroacoustic sensors, both by direct observation and from the literature.

The magnitudes of small seismic events M_1 recorded by hydroacoustic sensors in a water layer were generally determined from the duration of the seismic event τ (the duration of signals that remain at least 10% above the background level). To do this we used either the Brocher [25] equation $M_b = 2.30 + \log \tau$, or the Solov'ev–Kovachev calibration table [20]. The Brocher equation yields good estimates only for events lasting 100 s or longer. As we mostly had to deal with smaller events, the Solov'ev–Kovachev table was used for energy estimation.

For this table we determined a logarithmic regression line:

$$M_1 = 1.38 \ln(\tau) - 3.63, \quad (6)$$

for which the unbiased estimate of the determination coefficient was $R^2 = 0.9996$, that is, the residual variance controlled by the random component is very small. It should be noted that the hydrophone records of small seismic events that occurred far from the recording site were generally strongly distorted by noise, and the determination of signal period at maximum amplitude presented serious difficulties. It was for this reason that signal magnitude was derived from observations in the studies to

be referred to below using (6), which is based on the Solov'ev–Kovachev table.

K. Mogi [11] analyzes records of hydroacoustic signals made by a set of hydrophones on board a ship above the epicenter of an underwater earthquake. Events of magnitude of the order of $M = -3$, which were called elastic shocks, had periods of about 0.1–0.3 s. Mogi identified microearthquakes of three types, A, B, and C. Type A microearthquakes typically have durations of 1 to 1.7 s, with the figure for types B and C being 6–7 s. The magnitude of such a signal (M_1 as found from the Solov'ev–Kovachev relation) was determined to be -2.9 to -3.6 (for type A) and between -0.9 and -1.2 (for types B and C).

There are microearthquakes lasting 5 to 90 s, for examples consult [29]; the magnitudes M_1 for these were determined to be between -1.4 and $+2.6$. Unfortunately, it has not been found feasible to determine the signal frequency in the maximum amplitude phase for the signals presented in that study.

The small events described in [30], which are called nanoeearthquakes by the authors, (this name was first used in 1980, as far as we are aware) were recorded by hydrophones in water-filled wells in California near the San Andreas fault. The periods of the recorded signals were about 0.001 s, and the magnitude of that event as calculated by the authors with the help of extrapolation applied to some little known empirical formulas was estimated as being no greater than $M = -7$.

Sensitive seismographs have recorded [7, 23] small shocks with magnitudes about $M = -4$, the characteristic periods of the signals being 0.05–0.30 s. These studies and several earlier publications [13, 24] make it possible to construct a relationship of dominant period against earthquake energy.

In order to refine this relationship we carried out several series of hydroacoustic measurements using various hydroacoustic receivers deployed in various water areas off the Pacific coasts and special experiments in seismic areas of the Sakhalin–Kuril region.

The *first series* consists of data treated by these authors [17] and obtained from the deployments of self-contained ocean bottom stations (OBS) in Kamchatka, the Kuril Islands, the Sea of Okhotsk, and the Japan Sea. The station instrumentation includes scanning hydrophones to record motion in two ranges of frequency: 2–100 Hz and 100–1400 Hz (the continuous records lasted as long as 24 h).

The hydroacoustic records were analyzed to identify earthquakes and series of microearthquakes that preceded these. The durations of individual microearthquakes varied between 0.8 and 103 s, their magnitudes M_1 , given by (6), were found to lie in the range from -4.0 to $+2.8$. However, most microearthquakes (85%) had durations between 2 and 4 seconds (the respective values of M_1 were

between -1.8 and -2.8). The signal frequency content (in the maximum amplitude phase) was determined to be in the range 20 to 120 Hz.

The *second series of experiments* was the processing first applied by these authors to data from an AGAM hydroacoustic aerial [4, 9], which was a matrix of 2400 hydrophones. The aerial was submerged under water near the seafloor (6–10 m). We processed 162 hydroacoustic records each lasting 133.73 s; the sampling frequency was 300 per second; the input included a band-pass analog filter (40–110 Hz); the period of observation was 276 days [9, 12, 28].

An analysis of these records revealed two types of signal.

(1) Microearthquakes with acoustic signals in the range of 40–75 Hz, durations of 3 to 4 s, and very sharp amplitude jumps (a 20-fold increase in the amplitude of the hydroacoustic signal above the noise level was observed during the first 1–2 s). The high amplitude part of the signal has a frequency of 75–60 Hz; afterwards the period increases and the amplitude decreases. Microearthquakes usually occur in packets of 5–15 events following in succession with short time intervals between them, the events being generated by different, but closely spaced sources. The values of M_1 as found from the record duration τ varied in the range of -2.1 to -1.8 .

(2) Signals of the second type are signals from microfractures that are characterized by sufficiently large amplitudes comparable with the amplitudes of micro-earthquake signals, and show the tendency to occur in clusters. The duration τ of signals from microfractures is very short, a few hundredths of a second, so that the value of M_1 can be approximately estimated as lying between -10 and -8 . The high frequencies that are characteristic for these signals (over 110 Hz) have been truncated by the input band-pass filter.

Figure 1 shows: a sample hydroacoustic record that happened to be made at the time of an earthquake (fragment *a*), which occurred at the very end of the record; and two fragments *b* and *c* that have been stretched along the time axis and that contain the microearthquake and microfractures that the record contains in fragment *a*. The parameters of this earthquake are as follows: date, October 20, 1998; time, 03:15:46; energy class, $K = 10.3$; epicenter coordinates, 52.51° N and 158.07° E; depth of focus, 119 km; and the epicenter–seismometer distance, 50.4 km. Nine microearthquakes before the main event have been identified in fragment *a* (marked by triangular asterisks) and a series of microfractures (marked by arrows). The lower frequencies (below 40 Hz) were truncated by the input filter, so that the signal due to the earthquake itself has a small amplitude.

The *third series* consists of the data obtained by a team of researchers in Kamchatka [8]. Hydrophones were deployed in a lake or in a manmade reservoir, the hydroacoustic signals were continuously recorded by several

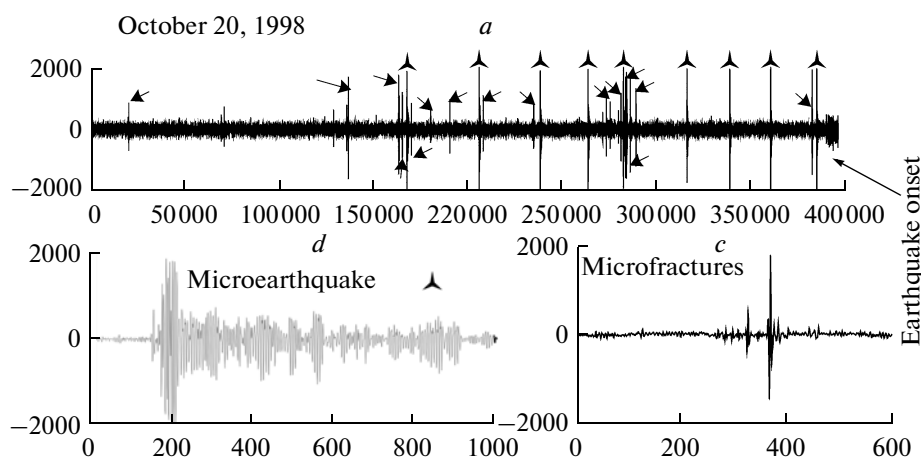


Fig. 1. A hydroacoustic record that contains nine microearthquakes and a series of microfractures, which coincides in time with an earthquake (fragment *a*); a segment of fragment *a* with a duration of 3.3 s containing a microearthquake (fragment *b*); a segment of fragment *a* with a duration of 2 s containing a series of microfractures (fragment *c*). The horizontal axes for all fragments show the time in sample points (300 samples per second), the vertical axes show the signal amplitude in mV. Fragment *a* lasts 1323.73 s (about 400 000 sample values). The microfractures are marked by arrows and the microearthquakes by triangular asterisks.

pressure-gradient receivers oriented along the cardinal points and downward in several frequency ranges (from 0.1–10 Hz to 3000–6000 Hz). Band-pass filters were used.

Patterns of chaotic behavior for the signals due to individual microfractures were recorded during the precursory period of earthquakes, but the seismic signal had its structure unchanged, so that the parameters of individual microfractures could be evaluated (source length, the depth to the source, and the energy characteristics of the signals). The mean signal duration was found to be 1.5×10^{-2} s; consequently, the value of M_1 could be estimated to lie approximately within the limits between -11 and -8 (based on relationship (6)), with the source depth H_S being between 3 and 20 m.

In the *fourth series of recordings* a station has been deployed in a closed reservoir near the town of Kholmok on Sakhalin I. since August 11, 2006 for parallel recording of seismic and hydroacoustic signals in order to detect pulses that were generated during the critical phase of earthquake precursory periods [10]. The hydroacoustic subsystem had two scanning hydrophones with the frequency range 1 to 70 Hz and a sampling frequency of 200 Hz. Seismic and hydroacoustic signals were synchronized; a total of five channels were recorded.

The recording of series of similar signals (wave trains) began using hydroacoustic channels in August 16, 2006 in the time interval 3:30:00 to 19:30:00 GT. A characteristic fragment of a hydroacoustic record containing a wave train is shown in Fig. 2a (the record was made on August 17, 2006, the fragment started at 01:30:40 and lasted 50 s); three signals are identified in this wave train (Fig. 2b, the fragment starts at 01:30:45 and lasts 2.5 s).

The number of signals in a wave train varied within wide limits (from 7 to 130). The first signals in a wave train have considerably greater amplitudes compared with the background value (by factors of 3–7). When in a quiet state, the background amplitude is stable. The high frequency components of the signal have been truncated, but the signal duration in a wave train can be estimated, and this is nearly constant within a train. Each signal in a wave train consists of a pair of coupled pulses having durations of about 0.075 and 0.1 s, respectively. The two pulses have a total duration of 0.2 s. The magnitude of an individual microfracture M_1 can thus be estimated as lying between -6 and -7 .

The *fifth series of recordings* was made by these authors on Kunashir I. in August and September 2007 in Lake Lagunnoe, not far from the Sea of Okhotsk shoreline. We used a Delta-Geon 02M digital recorder. The analog-to-digital converter in this recorder has 22-bit resolution, so that the records can be made in a sufficiently instantaneous, broad dynamic range. The sampling frequency is 250 Hz. We recorded both earthquakes that were identified by the Yuzhno-Kuril'sk seismic station (four events) and microearthquakes. The earthquake class on the Rautian scale [26] K_R varied between 9.2 and 11.7. The records were truncated in the tail segment, so that it was impossible to accurately estimate the record duration to get an estimate for M_1 .

Figure 3 shows fragment *a*, which is a hydroacoustic record of an earthquake; fragment *b* of 25 min duration, which contains a series of microearthquakes; and fragment *c*, a stretched record segment from fragment *b* containing several microearthquakes.

The microearthquake durations vary between 0.6 and 3–4 s, corresponding to estimates of M_1 magnitude

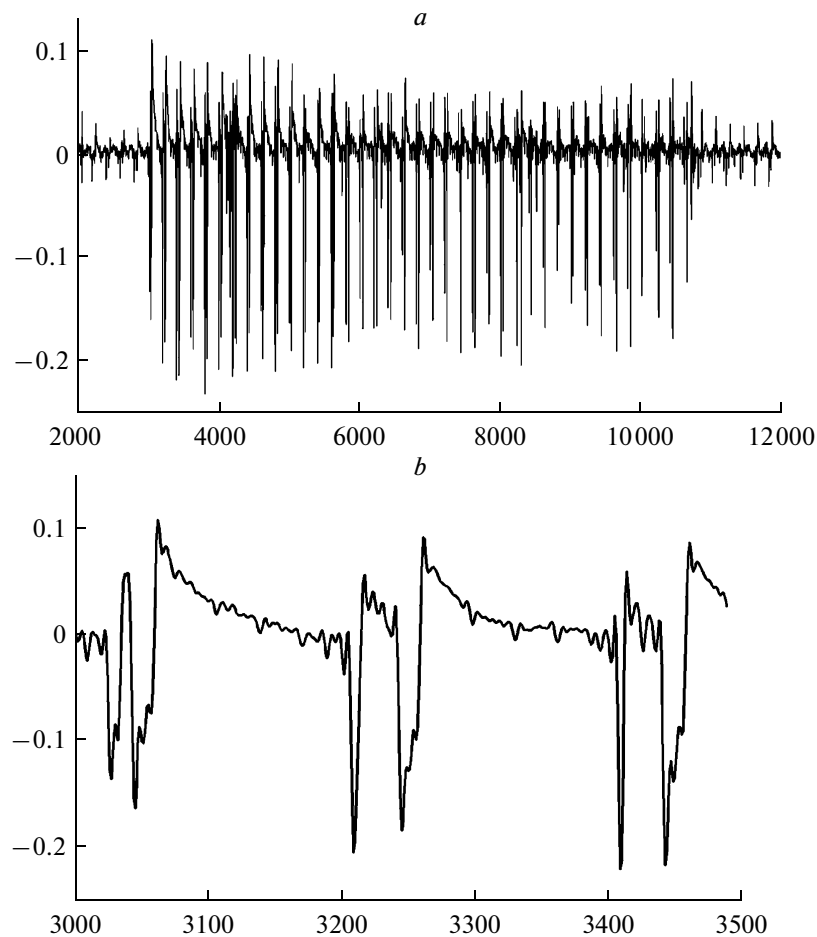


Fig. 2. A fragment of a hydroacoustic record with a wave train (*a*) and several signals in the earlier part of the wave train (fragment *b*). The horizontal axes for all fragments show the number of sample points (the sampling step was 0.005 s), signal amplitude in mV is plotted along the vertical axes. The example shown was taken from the record of August 17, 2006; fragment *a* started at 01:30:40 and lasted 50 s; fragment *b* started at 01:30:45 and lasted 2.5 s.

between -4.3 and -1.7 . The microearthquake records frequently have a complicated structure of interconnected pulses. The frequency range of the signals lies in the range 20 to 80 Hz.

The *sixth series of observations* was made by one of us (S.A. Borisov) on Sakhalin I. in the zone of an active fault 8 km from a mud volcano (20 km from the town of Yuzhno-Sakhalinsk). A hydrophone of sensitivity $200 \mu\text{V}/\text{Pa}$ was installed in a small lake. Signals were recorded using a microminiature recording system consisting of a 16-bit ADC and an built-in flash memory card.

Signals of geoacoustic emission are an uninterrupted chaotic sequence of pulses (microfractures). The main frequency components of the power spectrum are concentrated around ~ 360 and ~ 160 Hz.

Figure 4 shows fragment *a*, a hydroacoustic record of chaotically appearing microfractures (the fragment has a duration of 540 s); fragments *b* and *c* are individual signals of microfractures that have been identified in fragment *a*, these last fragments last less than 1 s.

The durations of signals due to microfractures vary between 0.18 and 0.035 s, corresponding to estimates of M1 between -6 and -8 . One characteristic feature of the recorded signals consists of their conspicuous high-frequency onset, with the signal subsequently decaying both an amplitude and frequency. Since the high frequency components are similar for all pulses, that may mean that the microfractures have approximately similar dimensions.

AN ANALYSIS OF EARTHQUAKE PARAMETERS AND SIGNAL ATTENUATION

In order to be able to estimate the parameters of these small earthquakes we brought the acquired materials of field observations together (see table) with source dimensions fixed in the range 0.01 cm to 10 km. For these dimensions we calculated the source volume ($V = L^3$) and energy using equation (1) (see columns 2 and 3 in the table). Columns 4 and 5 give the corresponding values of

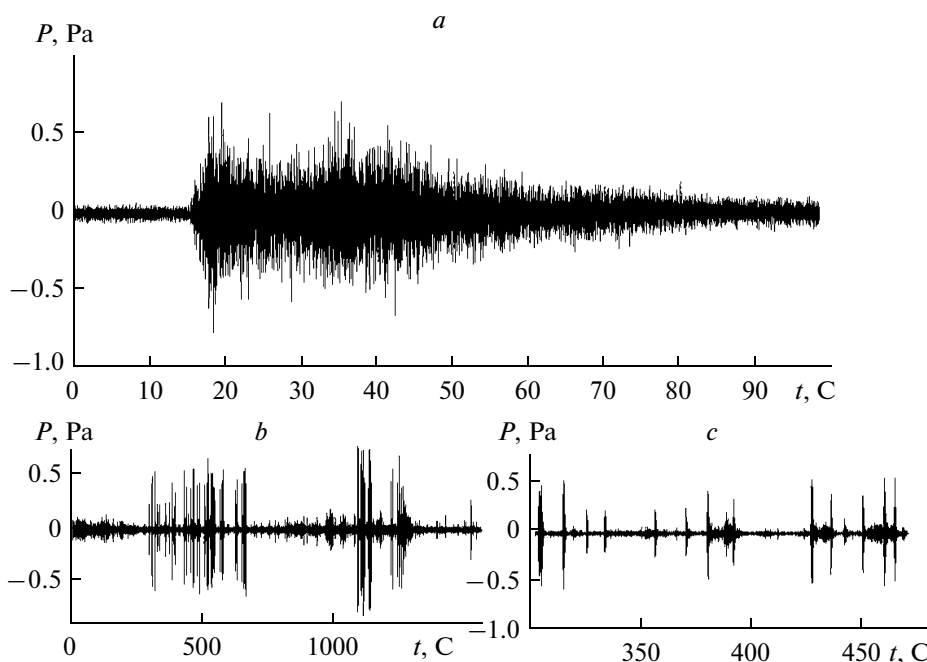


Fig. 3. Fragment *a* is a hydroacoustic record of an earthquake (no. 1511 as identified by the Yuzhno-Kuril’sk seismic station); fragment *b* has a duration of 25 minutes and contains a series of microearthquakes (the record started at 18:51:09 local time on August 12, 2007); fragment *c* is a segment of fragment *b* containing several microearthquakes starting from the 300th second. The axes of ordinates for all fragments show the time in seconds measured from the start of the record and the axes of the abscissas show pressure in Pa.

earthquake magnitude and energy class [3, 11, 20, 26] as given by

$$\log E = 1.5M + 11.8 \text{ (ergs)} \quad (7)$$

and

$$K_R = \log E \text{ (J)}. \quad (8)$$

We note that the Rautian energy class (K_R) was used here from considerations of convenience in estimating the energy of an event; the earthquake energy class by Solov’ev K_S that is used in the Sakhalin–Kuril region is related to the Rautian class as $K_R = K_S + 1.7$. The calculated value of the dominant period in a seismic signal radiated by a definite source (column 6 in the table) was obtained from (3).

We checked the resulting calculated period T and undertook a special study to examine the empirical data found in the seismological literature [14, 21], materials of our own hydroacoustic observations, and results from the processing of observations recorded at several stations of the Sakhalin Branch of Geophysical Service (GS) of the Russian Academy of Sciences (RAS). This analysis yielded a scatter diagram with the period of seismic signals plotted against energy (Fig. 5), the period values based on empirical data being entered in column 8 of the table.

Figure 5 also shows the linear fits due to Gutenberg and Richter from (4) [3] and to Kasahara [5] from (5), in addition to those obtained by ourselves. We note that the

relationship holds in a wide range of energy (from 10^3 to 10^{22} ergs). The empirical relationships

$$\log T = 0.15 \log E - 2.56 \quad (9)$$

and

$$\log T = 0.19 \log E - 3.0, \quad (10)$$

which were obtained from the Gutenberg–Richter formula (4) and that due to Kasahara (5) are quite consistent with the relationship we derived:

$$\log T = 0.17 \log E - 3.2. \quad (11)$$

Figure 6 shows a scatter diagram for seismic signal period versus magnitude based on observations at several stations of the Sakhalin Branch GS RAS (Yuzhno-Sakhalinsk YYS, Severo-Kuril’sk SKR, and Tymovskoe TYV), as well as a linear fit to the diagram: $\log T = 0.195 \log E - 3.2$, which is nearly identical with the Kasahara result (relationship (10)).

Comparison of the period values obtained by calculation and those based on the empirical relationship (11) (columns 6 and 8 in the table) yields quite satisfactory results and corroborates that the approach developed here is valid.

The relationship giving the period of a radiated signal as a function of earthquake energy (11) can be used to derive estimates of signal attenuation in rocks with different source energies and associated frequencies.

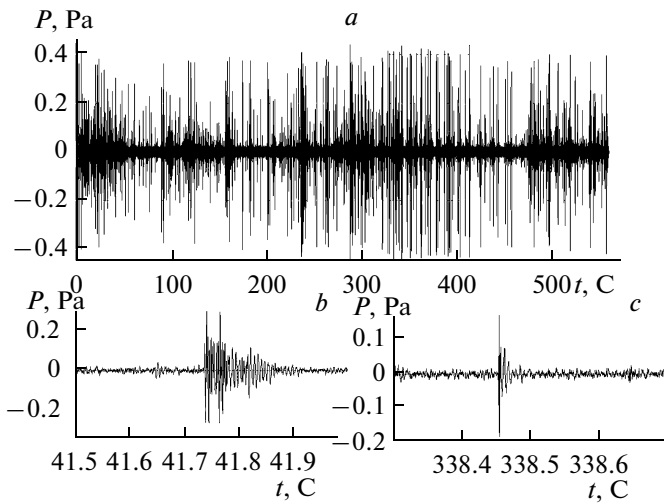


Fig. 4. Fragment *a* is a hydroacoustic record of chaotically occurring (in time) pulses of geoacoustic emission (the fragment duration is 540 s). Fragments *b* and *c* (both with durations below 1 s) contain individual signals from microfractures identified in fragment *a*. Fragment *b* contains two pulses and fragment *c* a single high frequency pulse. The axes of ordinates for all fragments show the time in seconds measured from the start of the record, the axes of abscissas give the pressure in Pa.

The attenuation of a signal as it travels through bedrock and sediments is controlled by energy loss in the rocks (intrinsic attenuation), geometrical spreading, and scattering. The attenuation of sound in a plane sound wave obeys the law [22]

$$I(x) = I_0 \exp(-\beta x), \tag{12}$$

where β is the energy attenuation constant, I_0 the wave energy at the source, and $I(x)$ the energy of the wave at a distance x from the source. The attenuation constant is measured in 1/m or 1/km. The intrinsic attenuation of signals in sediments and bedrock is proportional to the frequency: $\beta = k \times f$, where f is the frequency in Hz.

The attenuation constant k (1/km) is 0.0023 for bedrock, 0.0230 for sediments, and 0.1152 for sand [6, 22]. In

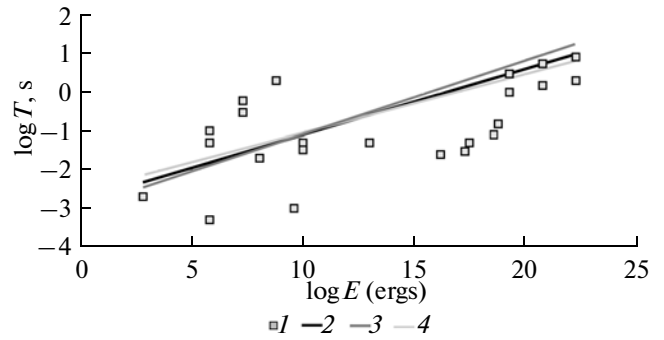


Fig. 5. Scatter diagram for the period of seismic signals versus energy ($T = f(E)$) based on observations and empirical functions for $T = f(E)$ in a log–log plot derived by several authors.

actual propagation of signals in complex media, because of multiple reflections at interfaces, one has to deal with mixed cases of combined spherical, cylindrical, and plane waves, hence the actual attenuation is much greater than is the case for plane waves. For seismic waves at source–receiver distances $x \geq 5 \times L$, where L is the linear size of the source, the wave propagates according to the spherical law.

Relationship (12) can be used to find the relative signal diminution ($I(x)/I_0$) due to attenuation as a function of the source–receiver distance. If more accurate methods applied in seismology were to be used, this would only increase the signal attenuation in real media.

Calculations show that when $f \geq 100$ Hz the wave is completely attenuated in a sedimentary layer less than 1 m thick. Under combined conditions it is only waves of frequency 200 Hz or less that can be transmitted through a layer of bedrock and sediments 0.5 km thick. Figure 7 shows log–log plots for the distances with 95% attenuation, separately for bedrock and sediments, under the plane-wave assumption.

Figure 8 shows plots of attenuation versus distance (on a log scale) for several frequencies. The solid dashed line

Earthquake parameters and the characteristics of radiated signals

Source length L , cm	Source volume V , cm ³	Source energy E , ergs	Earthquake magnitude	Earthquake class K_R , J	Signal period, theor., s	Signal frequency, Hz	Signal period, experim., s
1.00E – 02	1.00E – 06	1.00E – 03	–9.87	–10.00	2.0E – 04	5.0E + 03	2.00E – 04
1.00E – 01	1.00E – 03	1.00E + 00	–7.87	–7.00	6.3E – 04	1.6E + 03	6.31E – 04
1.00E + 00	1.00E + 00	1.00E + 03	–5.87	–4.00	2.0E – 03	5.0E + 02	2.00E – 03
1.00E + 01	1.00E + 03	1.00E + 06	–3.87	–1.00	6.3E – 03	1.6E + 02	6.31E – 03
1.00E + 02	1.00E + 06	1.00E + 09	–1.87	2.00	2.0E – 02	5.0E + 01	2.00E – 02
1.00E + 03	1.00E + 09	1.00E + 12	0.13	5.00	6.3E – 02	1.6E + 01	6.31E – 02
1.00E + 04	1.00E + 12	1.00E + 15	2.13	8.00	2.0E – 01	5.0E + 00	2.00E – 01
1.00E + 05	1.00E + 15	1.00E + 18	4.13	11.00	6.3E – 01	1.6E + 00	6.31E – 01
1.00E + 06	1.00E + 18	1.00E + 21	6.13	14.00	2.0E + 00	5.0E – 01	2.00E + 00

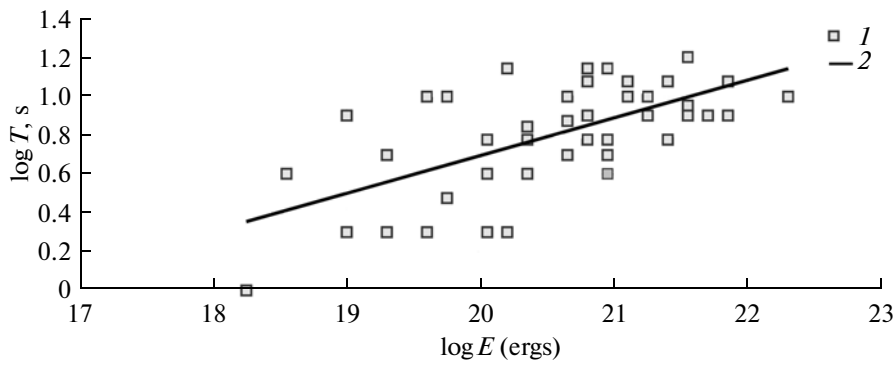


Fig. 6. Scatter diagram for the period of seismic signals versus energy ($T = f(E)$) based on observations at three stations in the Sakhalin region and the associated regression equation.

indicates 95% attenuation. It thus appears that signals with frequencies 200 Hz or higher cannot pass through the sedimentary layer alone. The above relationships for signal attenuation should be viewed as lower bounds on the maximum distance that a signal can travel before it is completely attenuated.

If our instruments record signals of geoaoustic emission at frequencies higher than 200 Hz, it follows that these signals must be generated in an immediate vicinity of the receiver, rather than arriving from the rupture of a future earthquake several tens of kilometers from the receiver. In the case where there is a time-dependent correlation between acoustic emission and earthquake precursory processes, then a change must have occurred in the state of the medium over large areas, and it is this which is recorded by the instrument.

DISCUSSION OF RESULTS

The foregoing analysis of the empirical relationship between dominant signal period and earthquake energy

(or magnitude) expands our knowledge of the earthquake source physics. Assuming that some limiting value of 3-D energy density exists in the rupture volumes of crustal earthquakes and that the total energy is proportional to the third power of linear source dimension (2), we are forced to represent the relationship between the signal period and source dimension as a relation, e.g., (3). Numerous observations in a wide range of energy corroborate the existence of a power-law relationship for $E(T)$ in the form (11) or, respectively, as

$$\log E = 6 \log T + 19.2. \tag{11a}$$

The above relationship is valid when the energy is in ergs. Expressing it in joules, we obtain

$$\log E = 6 \log T + 12.2. \tag{13}$$

Using the principles of dimension theory [2], some physical considerations will help construct a dimensionless complex that combines earthquake energy E , 3-D energy density $e = \rho g H$, and signal period $T = (L/g)^{0.5}$ in the form

$$\Pi = \rho g H L^3 / E = \rho g H (g T^2)^3 / E = \rho H g^4 T^6 / E.$$

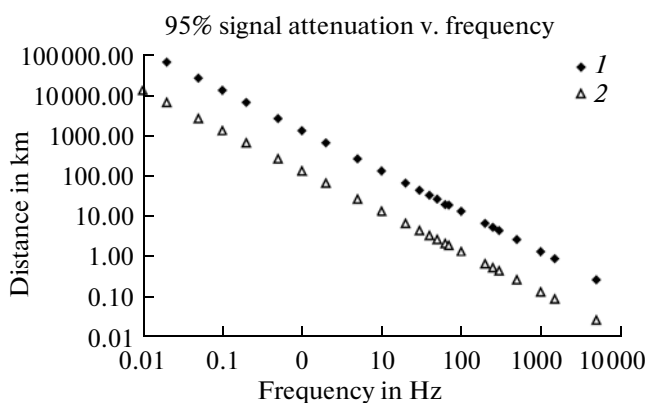


Fig. 7. Distance in km (from the source of signals) through which the signal is 95% attenuated as a function of frequency for bedrock and sediments plotted separately, assuming a plane wave. These are log-log plots.

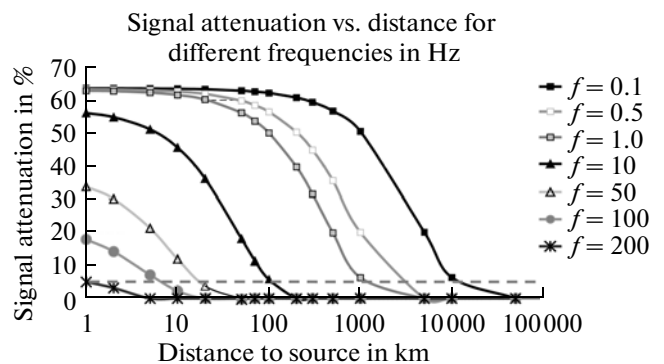


Fig. 8. Signal attenuation versus the distance to the source for several frequencies (on a log scale) for a combined medium (geometrical spreading incorporated). The solid dashed line marks the 95% attenuation (the remaining signal is 5% of the signal at the source).

Hence

$$E = \Pi_1 \rho H g^4 T^6. \quad (14)$$

Setting $\rho = 3 \times 10^3 \text{ kg/m}^3$, $g^4 = 10^4 \text{ (m/s}^2\text{)}^4$, $H = 3 \times 10^4 \text{ m}$, we find that $E = \Pi_1 \times 10^{12} T^6$. Comparison of this result with the empirical relationship (13) yields $\Pi_1 \approx 1$. It follows that the approach we are developing is physically sound. The above interpretation does not of course pretend to be the only possible option, but it provides means for the further development of a physical scenario for the phenomenon under study.

Now we shall compare the M1 magnitude estimates based on signal duration (τ) derived from an analysis of hydroacoustic observational data with the magnitudes M found from the frequency characteristics of signals in accordance with table and relationship (11). We note that the magnitude uncertainty is commonly ± 0.5 .

The estimate of M1 for the first series of observations (self-contained ocean bottom stations) is between +2.8 and -4.0, that for M is between -0.04 and -3.5. For the second series of observations (the AGAM aerial): M1 is between -1.8 and -2.1 and M between -1.6 and -2.7 for microearthquakes; for microfractures the estimates are -7 to -8 (M1) and from -3.2 (M). It should be noted that the frequencies higher than 150 Hz have been truncated in this experiment, this being a possible explanation for the difference in magnitude estimates. For the third series of observations (by the Kuptsov team, Kamchatka) the estimates of M1 are between -8 and -11 and that of M is between -9 and -11. As to the fourth series of observations, we had only the signal envelopes to go upon (the higher frequencies were not available), so it has not been possible to estimate the period from records. For the fifth series of experiments the estimate of M1 was between -1.7 and -4.3, and that of M between -2.5 and -2.8. For the sixth series the estimate of M1 was between -7 and -8, and that of M from -5.5.

A comparative analysis of the two magnitude scales for small events, which were calculated independently of each other and were based on different parameters (signal period and total signal duration) showed sufficiently good agreement, except in cases where some of the required parameters could not be derived from available records.

It should be noted that the division of small events into subclasses (small earthquakes, microearthquakes, microfractures or nanoeearthquakes) thus far does not enjoy a widely accepted terminology nor does it rest on formally defined quantitative criteria. Most authors just simply refer to microearthquakes or to nanoeearthquakes as being the name in fashion without formally discriminating between these concepts. Sasorova et al. [28] proposed to classify such events by whether they have been recorded by onshore sensors and by signal duration (τ). We recall that $\tau > 100 \text{ s}$ for small earthquakes, and such events can be recorded by stations installed on land. Microearthquakes ($1 \text{ s} \leq \tau \leq 100 \text{ s}$) and microfractures

($\tau \leq 0.1 \text{ s}$) are not recorded by stations installed on land (at the present time).

Considering that the capabilities of measuring instruments are ever-expanding, while the need for the study of low magnitude seismicity is always growing, it is necessary to develop a formal criterion to clearly distinguish these concepts. The estimation of earthquake parameters based on the total energy of an event as a function of earthquake source volume or length gives an idea of the energy characteristics of the event and the frequency features of the associated signal.

We propose the following boundaries for classifying such events into subclasses:

small earthquakes are events with magnitude $1 \leq M \leq 3$; the relevant parameters are signal frequency $3 \text{ Hz} \leq f \leq 10 \text{ Hz}$ and source length $10 \text{ m} \leq L \leq 100 \text{ m}$ (table);

microearthquakes are events with magnitudes between 0 and -4; the relevant signal frequency is $20 \leq f \leq 170 \text{ Hz}$ and the source length is $3 \text{ cm} \leq L < 800 \text{ cm}$; and

microfractures (or nanoeearthquakes) are events with magnitudes $M \leq -5$ and the parameters $f \geq 200 \text{ Hz}$ and $L < 3 \text{ cm}$.

We envisage a transitional (buffer) zone between small earthquakes and microearthquakes with magnitudes $0 < M < 1$ and the frequency range $10 < f < 20 \text{ Hz}$; a similar zone is envisaged between microearthquakes and microfractures: the magnitudes are $-4 < M < -5$ and the frequency range $170 < f < 200 \text{ Hz}$.

According to this classification, the energy of a small earthquake is between 2×10^{13} and 2×10^{16} ergs; for microearthquakes it is between 6×10^5 and 6×10^{11} ergs; for microfractures (nanoeearthquakes) it is below 2×10^4 ergs.

The preceding analysis of the data published previously and those first reported here permits us to refine the empirical relationship between earthquake magnitude and the period of radiated signals, helps us to develop a technique for reliable estimation of the magnitudes of small (high frequency) seismic events, and suggests a theoretical interpretation (14) of the empirical patterns of the seismic process considered here (based on dimension theory). These results can subsequently be used to deal with problems arising in regional seismogeodynamics.

ACKNOWLEDGEMENTS

This work was supported by the Russian Foundation for Basic Research (grant nos. 06-05-08098, 07-05-00142, and 07-05-02111). We are grateful to V.V. Adushkin and I.N. Tikhonov for helpful discussions, to G.A. Sobolev for valuable remarks, and to Ch.U. Kim and N.S. Kovalenko who kindly provided us with their observational material.

REFERENCES

1. Asada, T., Observations of Nearby Microearthquakes with Ultrasensitive Seismometers, *Phys. Earth*, 1957, vol. 5, pp. 83–113.
2. Barenblatt, G.I., *Podobie, avtomodel'nost', promezhutochnaya asimptotika* (Similarity and Self-Similarity, Intermediate Asymptotics), Leningrad: Gidrometeoizdat, 1982.
3. Gutenberg, B. and Richter, Ch.F., Earthquake Magnitude, Intensity, Energy, and Acceleration (II), *Bull. Seismol. Soc. Amer.*, 1956, vol. 46, no. 2, pp. 105–145.
4. Karlik, Ya.S., The Hydroacoustic Aerial—a Powerful Tool for Prediction of Tsunami-Generating Earthquakes, in *Lokal'nye tsunami: preduprezhdenie i umen'shenie riska* (Local Tsunamis: Risk Prevention and Mitigation), Moscow: Yanus-K, 2002, pp. 72–74.
5. Kasahara, K., On the Nature of Seismic Sources, *Bull. Earthqu. Res. Inst., Univ. Tokyo*, 1957, vol. 35, Part 3, pp. 473–514.
6. Clay, C.S. and Medwin, H., *Acoustical Oceanography: Principles and Applications*, New York: John Wiley & Sons, 1977.
7. Kocharyan, G.G. and Spivak, A.A., *Dinamika deformirovaniya blochnykh massivov gornykh porod* (The Dynamics of Deformation in Block Rock Massifs), Moscow: Akademkniga, 2003.
8. Kuptsov, A.V., Larionov, I.A., and Shevtsov, B.M., Geoacoustic Emission during Earthquake Precursory Periods in Kamchatka, *Vulkanol. Seismol.*, 2005, no. 5, pp. 45–59.
9. Lappo, S.S., Levin, B.V., Sasorova, E.V., et al., Hydroacoustic Location of the Generation Region of an Oceanic Earthquake, *Dokl. RAN*, 2003, vol. 388, no. 6, pp. 805–808.
10. Levin, B.V., Sasorova, E.V., Kim, Ch.U., et al., The August 17(18), 2006 Earthquake on Sakhalin I. and the First Implementation of a Multidisciplinary Forecast, *Dokl. RAN*, 2007, vol. 412, no. 3, pp. 396–400.
11. K. Mogi, *Earthquake Prediction*, Academic Press, 1985.
12. Morozov, V.E. and Sasorova, E.V., Preseismic High Frequency Signals (40–110 Hz) Inferred from Hydroacoustic Data on the Pacific Coast of Kamchatka, *Vulkanol. Seismol.*, 2003, no. 1, pp. 64–74.
13. Rykunov, L.N. and Smirnov, V.B., General Features of Seismic Emission at Different Time Scales, *Fizika Zemli*, 1985, no. 6, pp. 83–87.
14. Rykunov, L.N. and Smirnov, V.B., Microscale Seismology, *Vulkanol. Seismol.*, 1992, no. 3, pp. 3–15.
15. Sadovskii, M.A., Kedrov, O.K., and Pasechnik, I.P., On Seismic Energy and Source Volume for Crustal Earthquakes and Underground Explosions, *Dokl. AN SSSR*, 1985, vol. 263, no. 5, pp. 1153–1156.
16. Sasorova, E.V. and Levin, B.V., Low Frequency Seismic Signals as Regional Precursors of Earthquakes, *Vulkanol. Seismol.*, 1999, nos. 4/5, pp. 126–133.
17. Sasorova, E.V., Morozov, V.E., Lysenko, Yu.V., and Korovin, M.E., Hydroacoustic Monitoring of Seismic Events in the Ocean, in *Fundamental'nye issledovaniya okeanov i morei* (Basic Research in Oceans and Seas), Book 1, Moscow: Nauka, 2006, pp. 254–263.
18. *Slabye zemletryaseniya* (Small Earthquakes), Riznichenko, Yu.V., Ed., Moscow: Izd-vo Inostr. Liter., 1961 (This book contains the translations of 34 papers concerned with the title subject. References to particular papers are given where the paper is specifically mentioned: [[1, 5 23]]).
19. Smirnov, V.B., Estimating the Duration of the Fracture Cycle in the Earth's Lithosphere from Earthquake Catalogs, *Izv. RAN, Fizika Zemli*, 2003, no. 10, pp. 13–32.
20. Solov'ev, S.L. and Kovachev, S.A., On Determining the Local Magnitudes of Regional Earthquakes Based on OBS Observations, *Fizika Zemli*, 1996, no. 5, pp. 26–30.
21. Fedorova, I.V., Vandysheva, N.V., Golenetskaya, I.G., et al., The Analysis of P-Wave Records Made at Stations of the Unified Seismic Observation System in Connection with Magnitude Determination, in *Magnituda i energeticheskaya klassifikatsiya zemletryaseni* (Magnitude and Energy Classification of Earthquakes), vol. 1, Moscow: IFZ AN SSSR, 1974, pp. 154–162.
22. Sheriff, R. E. and Geldart, L. P., *Exploration Seismology*, Cambridge University Press, 1995.
23. Tsuboi, C., Earthquake Energy, Earthquake Volume, Aftershock Area, and Strength of the Earth's Crust, *J. Phys. Earth*, 1956, vol. 4, pp. 63–66.
24. Yudakhin, F.N., Kapustyan, N.K., Antonovskaya, G.N., and Shakhova, E.V., Identification of Low Activity Faults in Platforms Using Nanoseismic Technologies, *Dokl. RAN*, 2005, vol. 405, no. 4, pp. 533–538.
25. Brocher, Th.M., T-Phases from the Earthquake Swarm on the Mid-Atlantic Ridge at 31.6°N, *Mar. Geophys. Res.*, 1983, vol. 6, no. 1, pp. 39–49.
26. Rautian, T.G., Khalturin, V.I., Fijita, K., et al., Origins and Methodology of the Russian Energy K-Class System and Its Relationship to Magnitude Scales, *Seismol. Res. Lett.*, 2007, vol. 78, no. 6, pp. 579–590.
27. Sasorova, E.V. and Levin, B.W., The Low-Frequency Seismic Signal Foregoing a Main Shock as a Sign of the Last Stage of Earthquake Preparation or Preliminary Rupture, *Physics and Chemistry of the Earth (C)*, 2001, vol. 26, nos. 10–12, pp. 775–780.
28. Sasorova, E.V., Levin, B.W., and Morozov, V.E., Local Tsunami Warning Problem and the One of Possible Method of Its Solving, *Proc. 22nd International Tsunami Symposium*, Chania, Greece, June 27–29, 2005, Papadopoulos, G.A. and Satake, K., Eds., Athens, 2005, pp. 204–210.
29. Spindel, R.C., Davis, S.B., Macdonald, K.C., Porter, R.P., and Phillips, J.D., Microearthquake Survey of Median Valley of the Mid-Atlantic Ridge at 36°30'N, *Nature*, 1974, vol. 248, pp. 577–579.
30. Teng, T. and Henyey, T.L., The Detection of Nanoeearthquakes, in *Earthquake Prediction—An International Review*, Simpson, D.W. and Richards, P.G., Eds., AGU, Maurice Ewing Series, USA, 1981, pp. 533–542.29.